Deployable Low Cost Outdoor Aerial Surveillance System

Ashish Tanwer, Muzahid Hussain, Parminder Reel
Electronics and Communication Department
Thapar University

Email id : ashishtanwer@gmail.com, hussain.to.u@gmail.com , parminder.reel@gmail.com

Abstract
This paper presents the design of a dual controlled (manual as well as autopilot) Deployable Low Cost Outdoor Surveillance system. This model provides situational awareness by obtaining real-time information in outdoor applications. The aircraft is designed to have wingspan of less than 6 feet capable of carrying autopilot system and useful payload. This highly autonomous flight control system has high resolution camera and an onboard video transmitting device, which transmits high quality video with specified GPS points and altitudes. Sensors are able to detect man-sized objects. Innovative robust construction coupled with light weight and inexpensive hardware is used in the design of the airframe and avionics. These features allow the airplane to be operated even by unskilled users or via autopilot.

Keywords: Surveillance, Monitoring, Flight-control, Unmanned Aerial Vehicle, Autopilot, Human-detection, Airplane, Distributed Computing, Beagle-board.

1. Introduction

This paper consists of design and development of UAV based Surveillance System. The system can operate manually as well as automatically with Autopilot. Beagle-Board placed on-board and base-station computer in combination provides computing platform to our system. Beagle Board is used for lighter computing work. For overall view of our design approach, the system developed has been divided in design-subsystems, subsystem's domains, functionality and interconnectivity among them as explained in later sections of the paper.

2. Airplane Design Specifications

The Aircraft model named skip-pod is highly stable and light in weight. BALSA Wood is used to manually construct the frame and the body of skip-pod Airplane. Our model can operate during daytime only. We are using Y-CLARK type of structure in construction of wings that provides more strength and high stability to plane as compared to other structures [1]. Aircraft is so much stable, that even if engine fails during flight, we can safely land our aircraft without harming onboard equipments. The schematic of Airplane Design as shown in Fig 1 is designed in Pro-E.

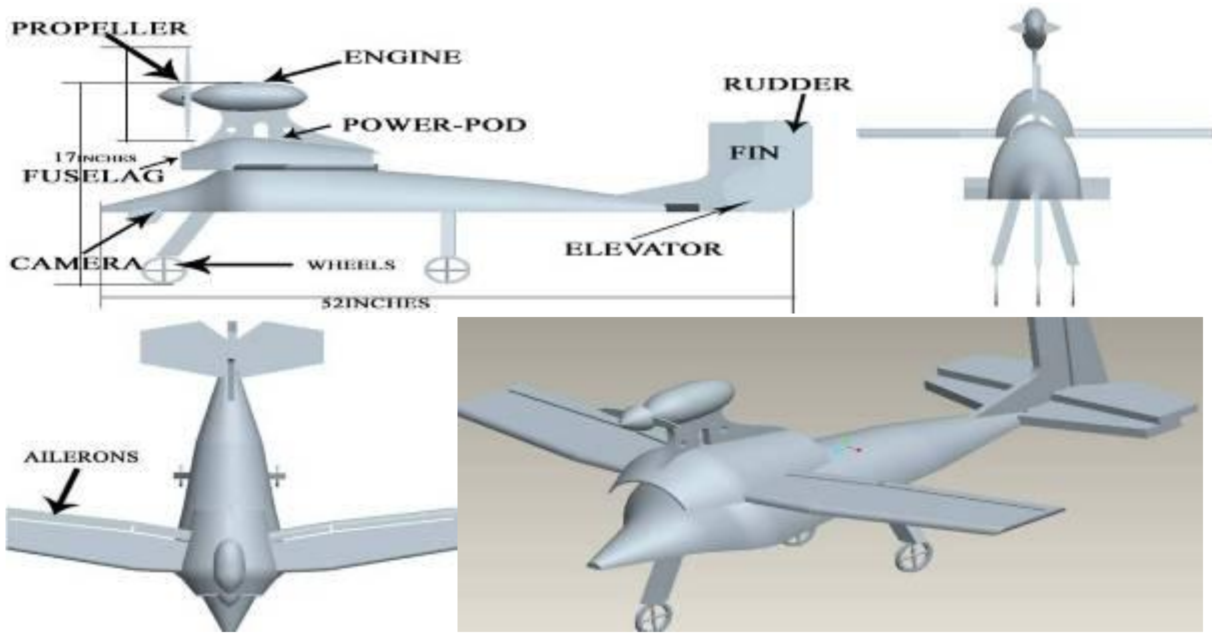

Fig1: UAV (a) Side View (b) Back-View (c) Top-View (d) 3D-View

The detailed technical specifications for airplane design are given in Table 1. We used OSMAX Japanese engine in our airplane. The specifications of the engine employed are described in Table 2.

Table 1: Airplane Design Specifications

Properties	Value
Wingspan (l X b)	70”inch X 10”inch
Airplane (l X h)	52”inch X 17”inch
Propeller height	12”inch
Tail (l X b X h)	10”inch X 5”inch X 12”inch
Front wheel position (uses one wheel)	15 degree inclined in front side & below starting of plane
Back wheesl position (uses two wheel)	Placed at 3/4 length of airplane
Power pod height from plane	4.5”inch
Centre of gravity (CGP)	3”inch from starting of plane
Wing Axes	2˚ inclined to provide stability
Weight (unloaded-loaded) of airplane	2.5kg & .5kg approx.
Speed	30 to 70 kmph

Table 2: Engine Specifications

S. No	PROPERTIES	VALUE
1	Displacement	10cc

2	Bore	22.0mm
3	Stroke	19.6mm
4	R.P.M (Practical)	2000-17000r.p.m
5	Weight	23.6oz
6	Propeller	12”inch x 6
7	Spinner	2”inch (turbo)
9	Silencer	120g/4.32oz
10	House power	1.9hp
11	Model	OSMAX (JAPAN)

Engine starts with Engine Igniter and runs on mixture of Methanol and Castor Fuel. We have dual control mode for our aircraft:

- ***Manual Control Mode:*** The Radio Control (RC) transmitter in our airplane has 6-Channel 72MHz FM Dual Radio control and 2 channels dedicated to AM Transmitter.
- ***Autopilot Control:*** Aircraft operates in Autopilot mode using onboard Autopilot Hardware along with sensors through the same RC transmitter [5].

We are using two types of RC transmitter in our aircraft model:

- ***FM RC transmitter:*** Transmitter with 6 channels is used to manually fly the UAV or to assist autopilot control such as during takeoff, landing and for remote throttle enable/disable for aircraft that may require the throttle off during launch. We are using the channel 5 switch on the RC transmitter to toggle the autopilot into RC Mode. RC Mode disables the autopilot’s autonomous modes and gives the user “dampened” RC control of the UAV using the RC transmitter, effectively “slowing down” the dynamics of the UAV. Turning ON RC Mode turns OFF autopilot control and vice versa.
- ***AM RC transmitter:*** It is 2-channel RC control used for controlling motion of camera in forward, backward, front and back side.

Reynolds number value for which our aircraft works properly is less than 2000. So, during flight it is stable for laminar and transition flow of air. Aircraft requires a 50m long runway for takeoff and landing.

3. Flight Control Design Logic

This Section describes details of the design of a flight control system to control and stabilize Aircraft. A Proportional Integral Derivative (PID) control structure is developed to stabilize and control the aircraft. To fly the aircraft autonomously, the autopilot must be capable of navigating waypoints. This requires that the autopilot be able to control the heading, altitude, and airspeed of the aircraft. In last sub-section we have discussed about flight control simulation and testing.

3.1 Manual Control

For manual control, it is desirable that the autopilot also accepts pitch and roll angle commands. To accomplish this, a controller constructed of nested PID loops has been developed. The aileron, elevator, and throttle commands are controlled via inner PID loops that stabilize the roll, pitch and throttle. The altitude and heading are controlled with outer loops, which produce commanded values for the inner loops.

3.2 Autopilot Control

The autopilot control is divided into two controllers:

- ***LATERAL CONTROL***: The lateral controller is responsible for controlling the yaw rate, roll angle, and heading. This is done with 3 inner servo loops and 1outer loop. [2] The inner loops produce efforts that drive the aileron and rudder. The outer loops produce commanded values for the inner loops.

The inner lateral loops are as follows:

i.***Aileron from Roll:*** This loop generates an aileron deflection from the roll error. This loop is responsible for holding the roll attitude of the aircraft.

ii.***Aileron from Roll Rate:*** This loop generates an aileron deflection from the roll rate. It is responsible for damping the roll rate of the aircraft. The control effort for this loop is summed with the effort from the Aileron from Roll loop and sent to the aileron servo actuator as shown in Fig 2.

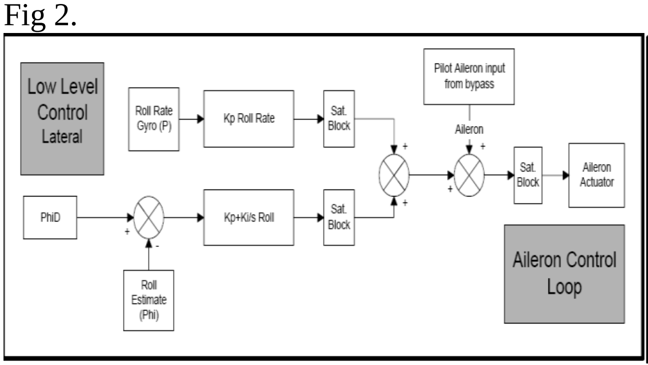

Fig 2: Inner Lateral Roll and Roll Rate Controller.

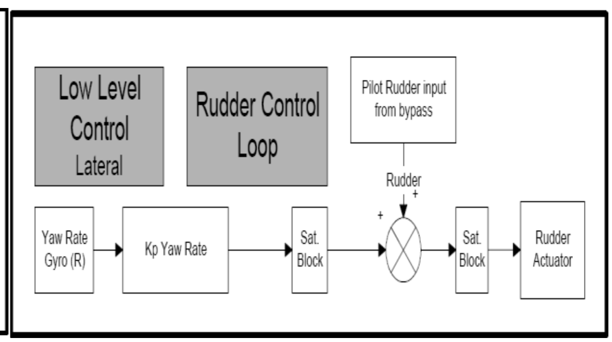

Fig 3: Inner Lateral Yaw Rate Controller

iii.***Rudder from Yaw Rate:*** The purpose of this loop is to control yaw rate of the aircraft. This loop drives the rudder servo as shown in Fig 3.

The outer lateral control loop is the following

iv.***Roll from Heading***: This is the loop responsible for controlling the heading of the aircraft. It generates a roll angle from the heading error. This roll angle serves as the commanded roll angle for the Aileron from Roll loop as shown in Fig 4.

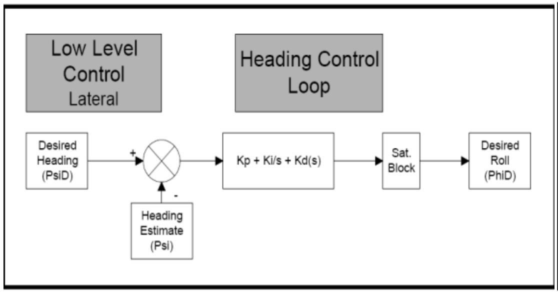

Fig 4: Outer Lateral Heading Angle Controller

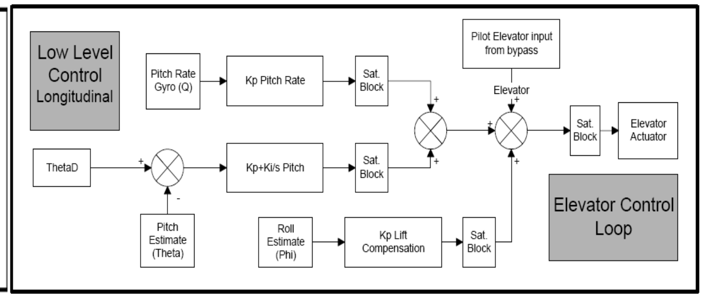

Fig 5: Inner Longitudinal Pitch and Pitch Rate Controller

- ***LONGITUDINAL CONTROL***: The longitudinal controller is responsible for controlling the velocity, pitch angle, and altitude. This is done with 3 inner servo loops and 2 outer loops. The inner loops produce efforts that drive the elevator and throttle [4]. The outer loops produce commanded values for the inner loops.

The inner lateral loops are as follows:

i.***Elevator from Pitch:*** This loop generates an elevator deflection from the pitch error. This loop is responsible for holding the pitch attitude of the aircraft as shown in Fig 5.

ii.***Elevator from Pitch Rate:*** This loop generates an elevator deflection from the pitch rate. It is responsible for damping the pitch rate of the aircraft. This loop's control effort is summed with the Elevator from Pitch loop and sent to the elevator servo actuator. (Fig 11).

iii.***Throttle from Airspeed:*** The purpose of this loop is to control the aircraft's airspeed by adjusting the throttle. This loop drives the throttle servo as shown in Fig 6.

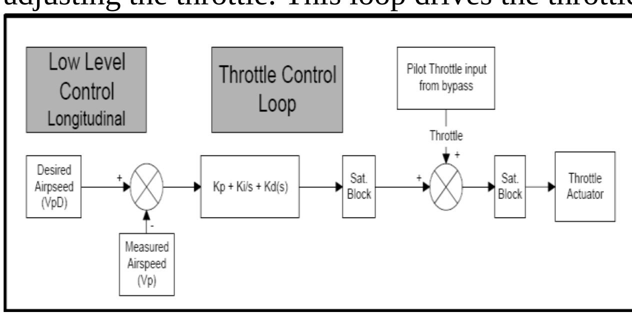

Fig 6: Inner Longitudinal Airspeed Controller

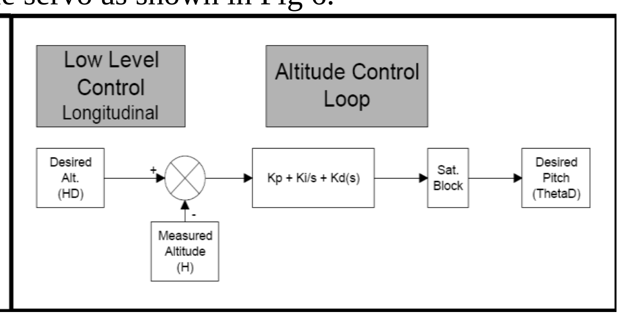

Fig 7: Outer Longitudinal Altitude Controller

The outer lateral control loops are as follows:

i.***Pitch from Altitude***: This loop generates a commanded pitch angle from the altitude error. The output of this loop connects directly to the Elevator from Pitch loop. This loop is ideal for controlling the aircraft's altitude when the altitude error is small. For large altitude errors, the Pitch from Airspeed loop should be used as shown in Fig 7.

ii.***Pitch from Airspeed:*** This loop controls the aircraft's airspeed by adjusting the pitch angle.

The output of this loop connects directly to the Elevator from Pitch loop. This loop is used to regulate the aircraft's airspeed during climb and descent as shown in Fig 8.

4. Aircraft Control Testing On Flightgear Simulator

Flight Gear is an open source aircraft simulator. We have tested Aircraft Control Commands by interfacing MATLAB (Aerospace Toolbox) with the FlightGear flight simulator to visualize and control motion of aircraft (flight data) in a 3-D virtual environment. We have made a unidirectional transmission link from the MATLAB (Aerospace Toolbox) to FlightGear flight simulator. Data is transmitted from MATLAB via User Define Protocol (UDP) network packets to a running instance of Flight Gear. The toolbox supports multiple standard binary distributions of Flight Gear 7. Fig 9 shown conceptual diagram of MATLAB aircraft simulation using aerospace toolbox.

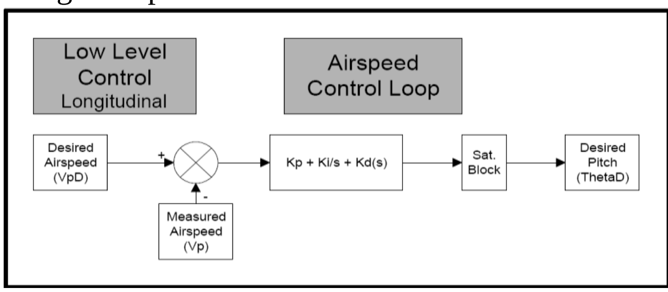

Fig 8: Outer Longitudinal Airspeed Controller

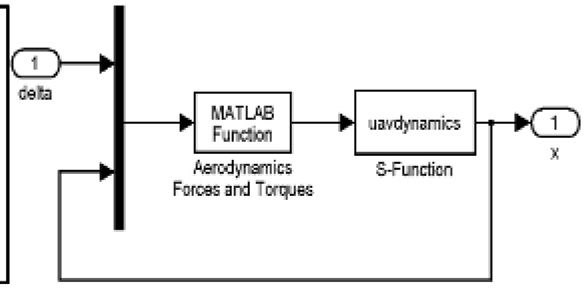

Fig9: The 6-Degree of Freedom MATLAB Aircraft Simulation

Steps to run virtual aircraft in Flight Gear simulator through MATLAB interfacing (refer fig 10):

1. Import the aircraft geometry into Flight Gear
2. Loading trajectory data: In this step, flight trajectory data for the flight simulation is loaded into MATLAB.
3. Creating a Flight Gear Animation object: Flight Gear Animation object is created by setting up the different properties like initial conditions (location and orientation), object properties, path trajectory and time scaling.
4. Create a run script for launching Flight Gear flight simulator.
5. Start Flight Gear flight simulator. In this step, virtual aircraft starts to follow the uploaded path trajectory.

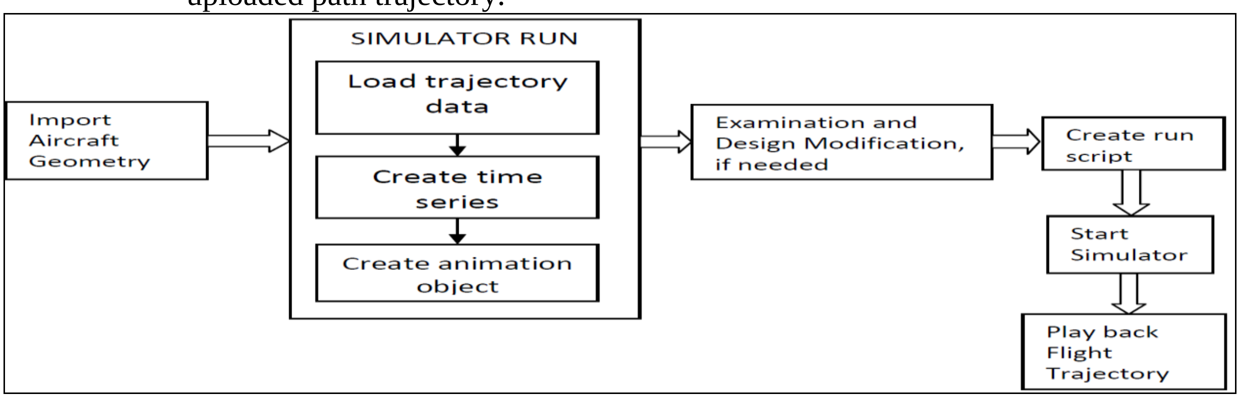

Fig 10: Virtualization of system in Flight Gear Simulator

6. On Board System

The onboard system can be divided into 3 subsections.

6.1 Avionics System

Basic Avionics System is shown in Fig 11. It consists of following subsections:

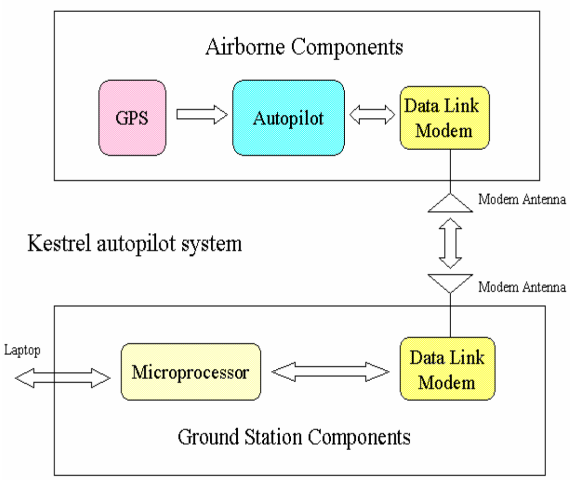

Figure 11 (a): Avionics system components

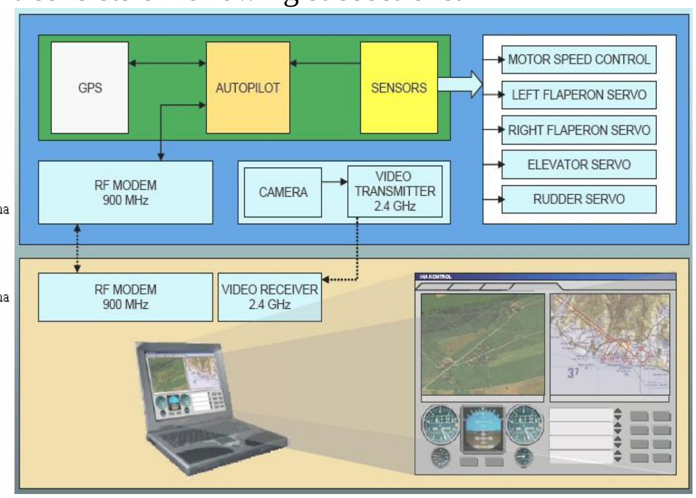

Figure 11 (b): Autopilot System Functioning

- ***Autopilot Processor Unit:*** The autopilot is operated by 8-bit 29 MHz Rabbit microprocessor and contains a sensors, 3-axis piezo gyros, accelerometers, and pressure sensors, used by the autopilot software to measure and estimate of the airplane attitude and location through the sensors as shown in Fig 12.
- ***Global Positioning System Unit:*** The Standard GPS presents velocity, heading, and position information, which is necessary for waypoint navigation with binary format. The GPS unit in the plane is passive and receives information via GPS satellite.
- ***Data Link Modem Unit:*** This modem allows real time communication with the ground station. A $\lambda/2$ dipole antenna is used on the aircraft. The autopilot helps communication with a digital modem running at 115 Kbaud. It supports a 57600 Kbaud over-the-air rate and a 1000mW power output [3]. Communication ranges of larger than 10 kilometers can be attained. The Data link antenna operates at a spread spectrum of 900 MHz and transmits real-time navigation data as well as other various airplane operations to a ground station [2].

The autopilot interfaces directly to the modem, which enables it to send real-time status telemetry to the ground station while receiving commands during the flight. Also it controls the servos that control the aircraft.

6.2 Payload Sub-System

Payload Sub-System consists of following subsections:

- ***Cmos Camera/Sensor Unit:*** The Sensor fitted below engine Cowl (*Refer, fig 1*), is active-pixel sensor (APS) consists of an integrated circuit containing an array of pixel sensors, each pixel containing a photo-detector and an active amplifier. Sensor is produced by a CMOS process (and is hence also known as a CMOS sensor), and has emerged as an alternative to charge-coupled device (CCD) imager sensors. The APS pixel solves the speed and scalability issues of the passive-pixel sensor. They consume far less power than a CCD, have less image lag, and can be fabricated on much cheaper and more available manufacturing lines.

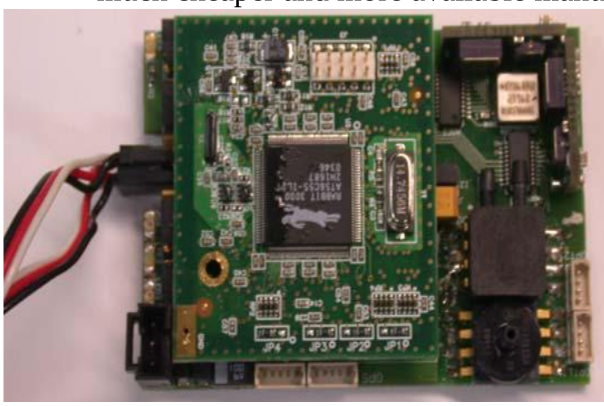

Fig 12: Autopilot Unit

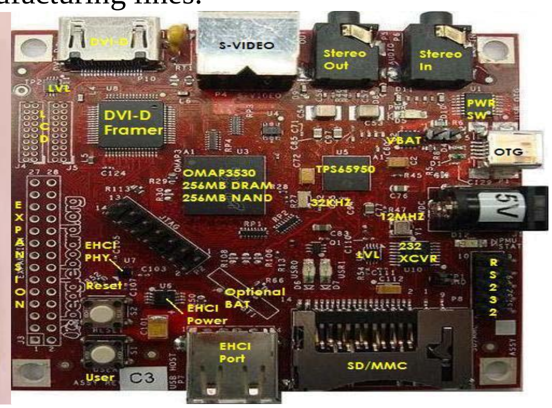

Fig 13 Beagle Board Payload

- ***Beagle Board Payload:*** We are using Beagle Board (Fig 13) a low-power, low-cost Single-board computer produced by TI, and interfacing it with sensors and display unit using Angstrom Linux as OS and Intel's Image Processing Library OpenCV. The purpose of this OpenCV program is to teach a computer to classify plants via their leaves. Various Image and Data Processing Techniques have been implemented for automated Object Recognition and classification as discussed in Section V.
- ***Video Transmitter Unit:*** The Video Transmitter used is 500mW, 2.4 GHz transmitter. The system is capable of a range greater than 5 km when an Omni directional antenna is employed on the receiving side.

Type	Radiation Pattern	Characteristics
Monopole GP Antenna 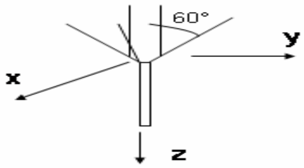	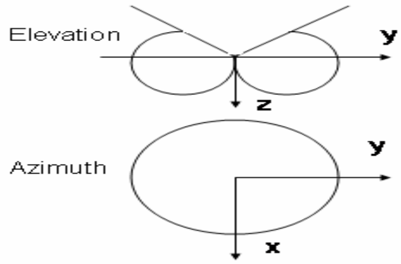	Typical Gain:2-6dB Polarization: vertical ,linear
λ/2 Dipole 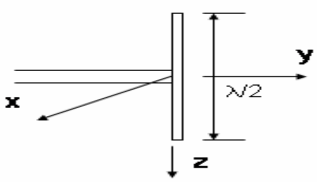	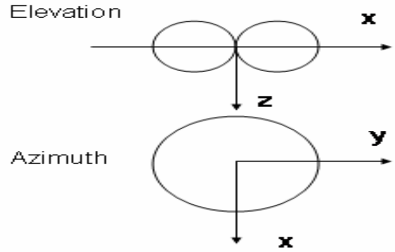	Typical Gain: 2-3dB Polarization: vertical ,linear

Fig 14: Comparison of antenna radiation pattern

- ***Video Transmitter Antenna Unit:*** A video-transmitting antenna operates at 2.4 GHz and transmits real-time video to the ground station. Most of the commercial video transmitters come with wavelengths (W) of the order λ/2 dipole and monopole antennas that are designed to have symmetric radiation patterns for getting rid of dead spots during the airplane's flight. Despite the transmitter's high output (more than 1 watt) and symmetric radiation pattern, the ground station frequently loses video signal. The GP antenna provides a bigger circle and downward pattern that provides a wider and more accessible region within which the airplane can fly without experiencing any dead zones (Refer Fig 14).

7. Video Data Processing

Once the Video is received at the Ground Station, Data Processing takes place. The data processing i.e. video processing consists of 4 steps for moving object detection and tracking.

- Reliability-Based Motion field vectors of the UAV video are estimated.
- Global vehicle-camera motion from these motion field vectors is derived.
- After stabilizing the video frame, we segment the regions of independent motion and then detect/track moving objects.
- Finally Moving Objects are classified using characteristics pertaining to individual object as person or vehicle.

These steps are described in detail as follows:

7.1 Reliability-Based Motion Field Estimation

We are using a simple distance measure, called SAD (sum of absolute difference) to estimate the motion vector for a large number of video frame blocks. We then analyze the reliability of motion estimation of each block [7]. Based on these motion vectors and their reliability information, we are able to determine the global vehicle-camera motion.

Let $\{B^m|1 \le m \le M\}$ be the group of structure blocks we extract from a video frame. For each structure block we find a subgroup of B^m consists of the best L matches found in the reference frame. By default L = 32. We denote these matches by $\Delta = \{(V_j^m, d_j^m)|1 \le j \le L\}$, where $V_j^m = (x_j^m, y_j^m)$ represents the motion vector $\vec{V}$ and d_j^m is the corresponding Sum of Absolute Difference SAD measure. Here $d_-^m = \min_j d_j^m$ and $d_+^m = Ave(d_j^m)_j$.

The idea here is that we use the distribution of motion vectors as the reliability measurement. Suppose V^m is the accurate or true motion vector, then there should be other vectors we found with SADs closed to V^m. It is obvious that the more these motion vector heading different direction the more uncertainty we have. On the other hand, even we have only few best matches (with low SAD), the diversity in their direction also cause mismatches. To define the reliability measure we further choose the best few matches by setting a threshold $d_0^m = d_-^m + \alpha.(d_+^m - d_-^m)$. By default α = 0.1 chosen between 0 and 1. The physical meaning of α is noise level. With the threshold now we define another subset of best few matches by:

$$\Delta_- = \{(V_k^m, d_k^m)|d_k^m \le d_0^m\} \tag{1}$$

V^m is the mean motion vector of the subset Δ_- which is labeled by index k and $1 \le k \le K^m \le L$.

$$V^m = \frac{1}{K_m}\sum_{k=1}^{K^m} V_k^m \tag{2}$$

The reliability measure is then defined as

$$\gamma^m = \frac{1}{1 + \sum_{k=1}^{K^m} \left\| V_m^k - V^m \right\|^2} \tag{3}$$

In a reliable case, either the motion vectors are close to each other (with less uncertainty or outliers) or the best matches are few. Both leads the reliability measure close to one ($0 < \gamma^m \le 1$).

7.2 Global Vehicle Camera Motion Estimation

Now based on the estimated motion vectors and the associated reliability measure for all structural blocks, we are able to determine the global motion parameters using weighted LMSE (least mean squared error) estimation for the video frames. As video frame has its own coordinate system, with respect to different angle of view [8]. An object in the scene which corresponds to pixel (x, y) in Frame B could correspond to another pixel (X, Y) in Frame A due to vehicle camera motion. This type of global motion caused by vehicle camera move could be modeled by a homographic transform:

$$\begin{bmatrix} X.W \\ Y.W \\ W \end{bmatrix} = \begin{bmatrix} h_{11} & h_{12} & h_{13} \\ h_{21} & h_{22} & h_{23} \\ h_{31} & h_{32} & h_{33} \end{bmatrix} \begin{bmatrix} x \\ y \\ 1 \end{bmatrix} \tag{4}$$

Where $W = h_{31} * x + h_{32} * y + h_{33}$ Rewriting above equation as

$$\begin{bmatrix} x & y & 1 & 0 & 0 & 0 & -x.X & -y.X \\ 0 & 0 & 0 & x & y & 1 & -x.Y & -y.Y \end{bmatrix} \begin{bmatrix} h_{11} \\ h_{12} \\ h_{13} \\ h_{21} \\ h_{22} \\ h_{23} \\ h_{31} \\ h_{32} \end{bmatrix} = \begin{bmatrix} X \\ Y \end{bmatrix} \qquad (5)$$

Each pair of coordinates (x, y) and (X, Y) can contribute to two rows in the left hand side matrix in the above equation. For each structural block, we use the block center position as (x, y) and the center position of its best match in the previous frame as (X, Y). The difference between (x, y) and (X, Y) gives the motion vector. Given the motion vectors and (x, y)-(X, Y) correspondence for all structural blocks, we can determine the global motion parameters **H** using Least Mean Squared Error (LMSE). Note that each (x, y)-(X, Y) correspondence is associated with a reliability measure γ^{m}. We can use γ^{m} as weighting factors to perform weighted LMSE. In this way, more accurate motion vectors have larger impact on the final estimation than those less accurate ones.

7.3 Moving Object Detection And Tracking

For Moving Object Detection, we segment regions of independent motion. The set of aerially shot video sequence frames It are first spatially Gaussian filtered to reduce noise (due to weather conditions), resulting in I_t*. The image I_t* is then stabilized with respect to image I_{t-T}*, resulting in $V_{t, t-T}$. The images $V_{t, t-T}$ and I_t* are differentiated and thresholded to detect regions of motion, resulting in a binary motion image:

$$M_{t,-T} = \begin{cases} 1 \;\; if \;\; \left| I_t^{*} - V_{t,t-T} \right| \; > \; T_M \;\; , \\ 0 \;\; otherwise \end{cases} \qquad \mathbf{(6)}$$

where T_M is a threshold. In order to eliminate false motion at occlusion boundaries (and help filter spurious noise), the motion images spurious noise $M_{t, T}$ and $M_{t, -T}$ are logically anded together:

$$M_t = M_{t,-T} \wedge M_{t,T} \qquad \mathbf{(7)}$$

Note that for small value of T (T =500 ms), motion parallax and a violation of the affine motion model that causes false motion in M_t . This technique has been extended to integrate multiple images differences. It provides more robust motion estimation than only using 3 images as above. The Simulink based implementation of our approach is shown in Fig15.

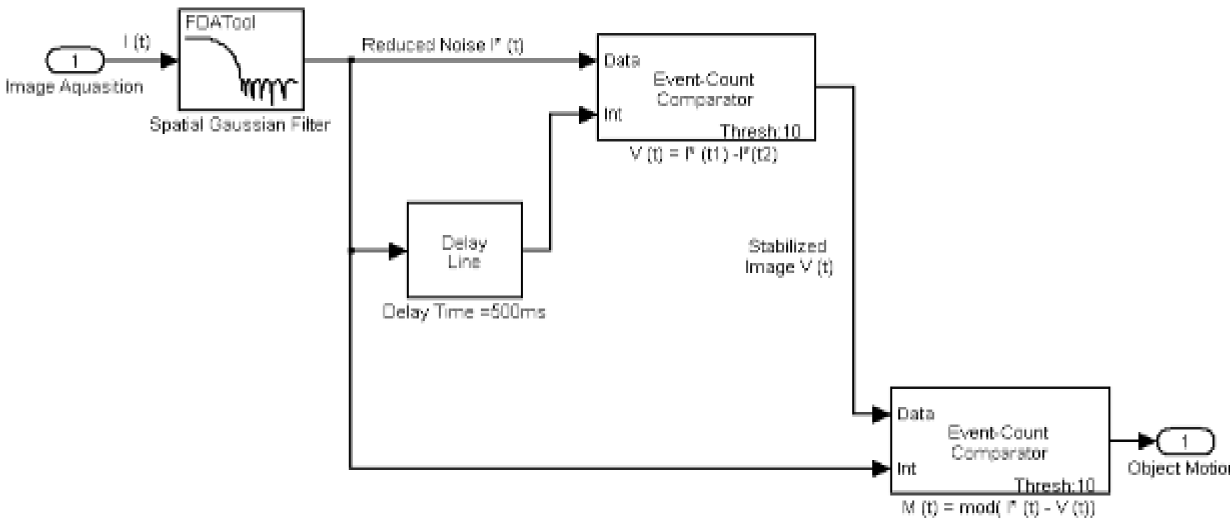

Fig15: Simulink model for Equations for Moving Object Detection

Applying morphological open operation on M_t (motion video frame can further reduce the motion due to noise from the aerial video frames. The connected components of M_t^* (open operated M_t) are computed and small components are eliminated (further reducing image noise). The connected components that are spatially similar (in distance) are then merged, and the merged connected components are added to a list of objects O_t to be tracked. An object can have the following attributes: area, centroid, bounding box, velocity, ID number, and age (in frames). Objects in O_t and O_{t+k}, $k > 0$, are corresponded using spatial and temporal coherence.

7.4 Object Classification

The moving objects detected in the last step are categorically classified using various factors. While object classification in aerial videos is particularly difficult due to image noise, Low GSD (Ground Sampling Distance), Poor Contrast, Motion Parallax, Motion Blur, and Camera Jitter due to aircraft motion.

Tracked objects are classified as people, vehicle, or other, using the object size, ground speed and periodicity of motion. An object's size is measured in ground are (computed using the image are and the estimated image to site-model registration). Since, a detected object may be fragmented into many blobs, the object size only used to help identify vehicles, but not people. Similarly, the ground speed is also only used to help identify vehicles, but not people, since vehicles can move slowly (like people), but people cannot typically run faster than 30 kms/hr. Mostly periodicity of the object's motion is the only attribute utilized to classify people.

8. Ground Observation

Observation at ground level is divided into two parts :

8.1 Ground Station Hardware

The purpose of the ground station hardware is to control and monitor the UAV and payload. The ground station hardware is enclosed in Fig 16. The ground station hardware can be divided into 4 sub-systems.

Fig 16: Ground Station Hardware

- ***Laptop:*** A laptop computer running Microsoft Windows is used. An in-house graphical user interface controls the autopilot.
- ***Autopilot-Specific Hardware:*** The digital modem at the ground station communicates with the digital modem in the UAV. A matching digital modem having 5 km range without the use of directional antennas, it has ¼-wave Omni-directional antenna which is used as the ground station communication antenna.
- ***Payload-Specific Hardware:*** The payload-specific portion of the ground station consists of the ground-based hardware necessary to make use of the payload carried by the UAV. In video surveillance payload, a video receiver, radio control transmitter, antenna, and video display are needed. The TV TUNER card receiver receives the video from the airplane. A high-gain directional patch antenna is used to achieve a 5 km range. A Laptop is used to display and record the video. During manual control, all controlling of airplane is done by RC transmitter.
- ***RC Transmitter Hardware:*** RC Transmitter with 6 channels is used to manually fly the UAV or to assist autopilot control such as during takeoff, landing and for remote throttle enable/disable for aircraft that may require the throttle off during launch. Use the channel 5 switch on the RC transmitter to toggle the autopilot into RC Mode. RC Mode disables the autopilot's autonomous modes and gives the user "dampened" RC control of the UAV using the RC transmitter, effectively "slowing down" the dynamics of the UAV. Turning ON RC Mode turns OFF autopilot control and vice versa. Refer Fig 17 for Detailed UAV system diagram.

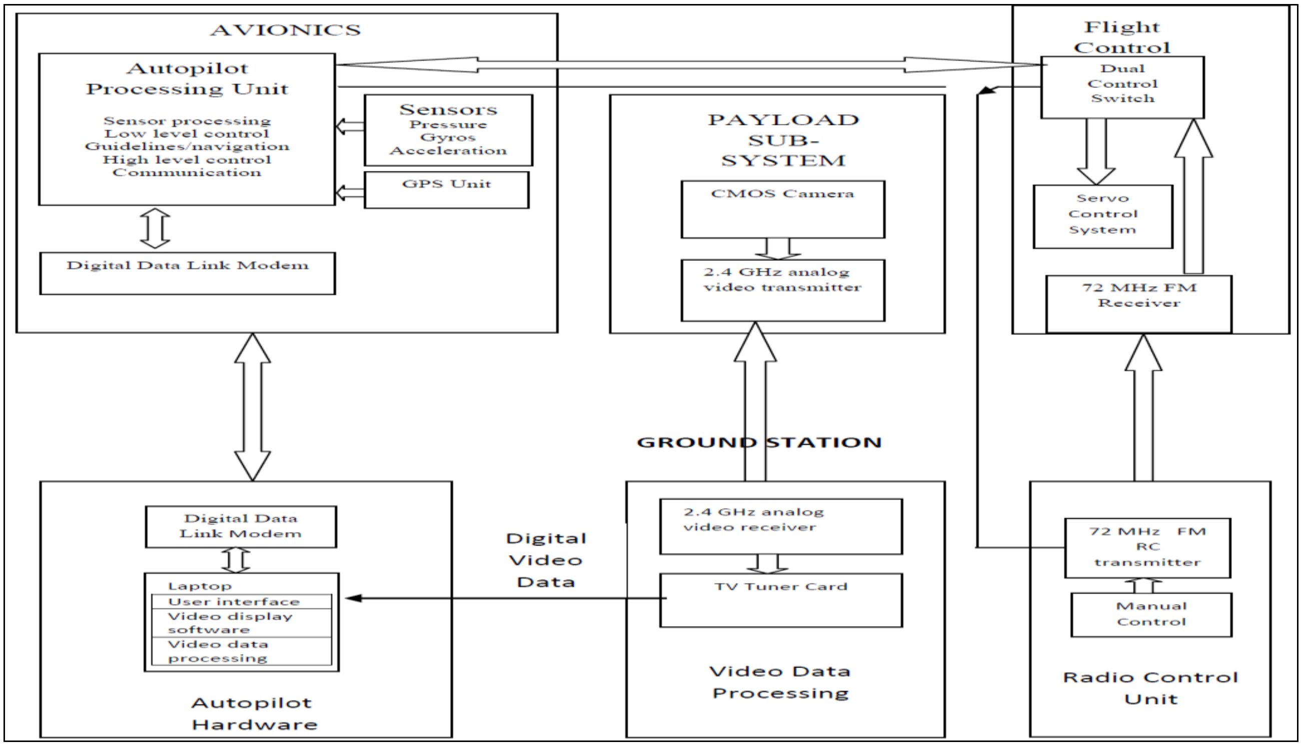

Fig 17: UAV System Diagram

8.2 Ground Station Software

A graphical interface has been designed to control the autopilot. The graphical interface software is known as the Virtual Cockpit. The Virtual Cockpit is a complete system that is used to configure, debug, program, and monitor the autopilot.

- ***Virtual Cockpit:*** The Virtual Cockpit contains several screens accessible by tabs and a Status screen that is always visible. The purpose of the Status window is to give the user an indication of the aircraft's status and health. The Virtual Cockpit has four tab windows, which contain specific control and setup information. Schematic of virtual cockpit main window is enclosed in Fig 18.
- ***Status Window:*** The Status window shown in Fig 18 is always visible and contains a collection of vital aircraft status information. The purpose of the Status window is to give the user an indication of the aircraft's status and health. The Status window is divided into two windows:

    - Attitude Indicator: The attitude indicator is a visual representation of the aircraft's pitch, roll, and heading. Heading information is displayed on the centerline of the attitude indicator, while pitch and roll can be derived from the location of the "horizon" as seen from the plane.

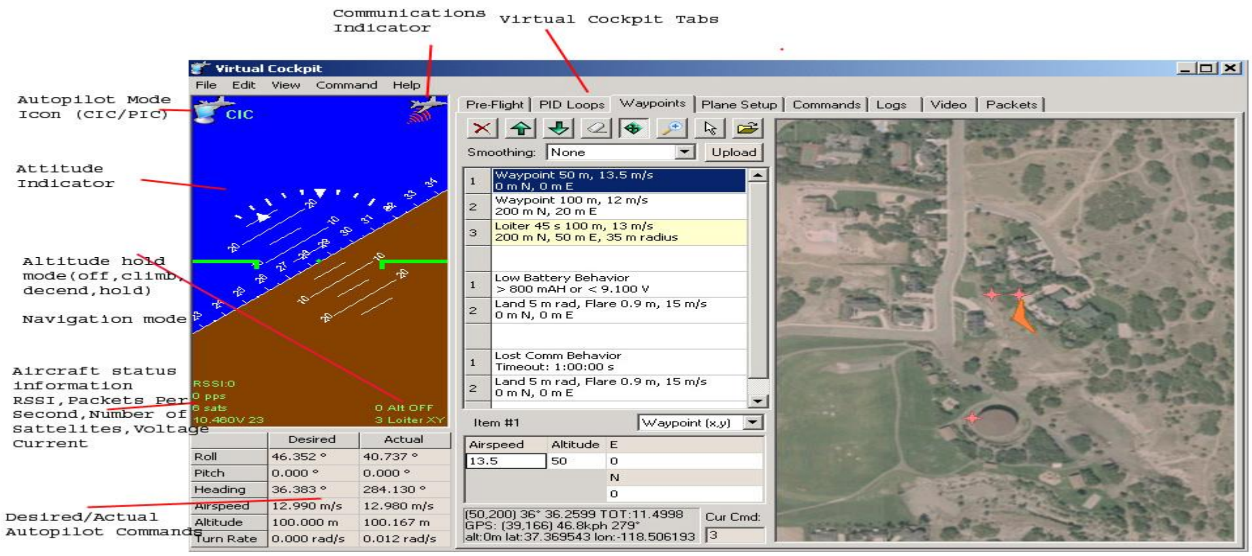

Fig 18 Ground Station Software

- ***Autopilot Mode:*** The upper left corner displays the autopilot mode. The autopilot has two modes:
  a. ***Pilot-In-Command (Pic) Mode***: In PIC mode, the autopilot actuator outputs are disabled and the aircraft is controlled either via the stick positions of the RC controller plugged into the ground station. The autopilot does not control the aircraft in this mode.
  b. ***Computer-In-Command (Cic) Mode:*** In CIC mode, the aircraft is commanded by the control efforts generated by the autopilot. Pilot inputs into RC controller plugged into the ground station, are summed into the autopilot control efforts. This is useful in autopilot gain tuning and development as it provides a method to test disturbance rejection by giving the pilot some control over the aircraft even when the autopilot is enabled. The pilot inputs can serve as disturbance inputs as well as control inputs. The mode is controlled by the channel 5 switch on the RC transmitter. If the channel 5 pulse is longer than 1500 µsec, the autopilot switches to CIC mode. If the channel 5 pulse is shorter than 1500 µsec, the autopilot switches to PIC mode. In addition to this it is also providing real time servo control window, attitude control window, map window and navigation status window to us. Fig 19 shows the overview of our operational system design and its functioning.

9. Conclusion

The above Design of a Low Cost Outdoor Surveillance System has been tested successful during DRDO Golden Jubilee Celebration Student Competition, a National level UAV design contest organized by DRDO, Govt. of India and won the first prize. The unique built of the aircraft provides a stable flight both in manual as well as autopilot controlled mode. We believe the airplane performance fits within the imposed design and application requirements. The airplane aerodynamic efficiency is designed to be most efficient for moderate speeds (as needed for video data capturing). The video processing algorithms used in video data processing are efficiently working on real time aerial videos and we have successfully identified human (like for

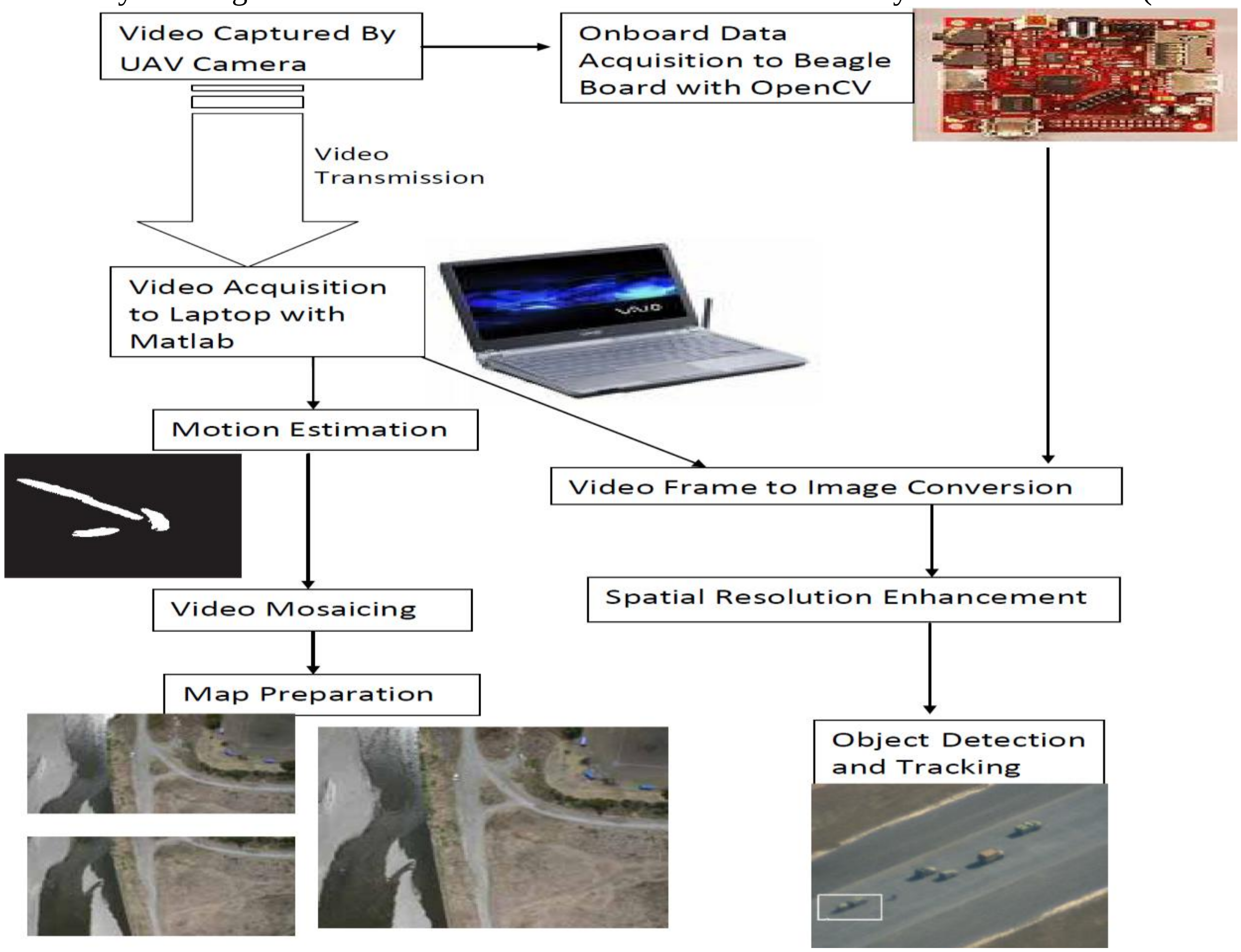

Fig 19: Overview of System Design and Functioning

a group of people walking or running on foot etc) from a height of 100m-500m. Specific tracking models have been developed for suspicious or random movements of vehicles/people. The airplane was designed not only around flight and application requirements, but also around an inexpensive price range. The plane cost is definitely much less then it counterparts seeing the wide range of the functionality and applications it can pursue.

References

[1] P. Raymer, Daniel "Aircraft Design: A Conceptual Approach" Published by American Institute of Aeronautics and Astronautics, inc. 370 L'Enfant Promenade, S.W., Washington, D.C. 20024 structures," in *Proc. IASTED Int. Conf. Robot. Appl.*, Honolulu,HI, Aug. 14–16, 2000.

[2] L. Ma and Y. Chen, “Aerial Surveillance System for Overhead Power Line Inspection,” Center for Self-Organizing and Intelligent Systems (CSOIS), Utah State Univ., Logan, Tech. Rep. USU-CSOIS-TR-04-08, Sep. 2000

[3] Xiaoyong Ye; Yong Lei; Haijun Hou, “Design Of Intelligent Mobile Vehicle System And Its Global Optimal Path Planning”, IEEE international conference on industrial technology, 2008.

[4] Long, L.N., “Computing, Information, and Communication: The Fifth Pillar of Aerospace Engineering,” Journal of Aerospace Computing, Information, and Communication, (www.aiaa.org/jacic), Vol. 1, No. 1, 2004.

[5] Srinivasan, S., and Latchman H., "Airborne Traffic Surveillance Systems – Video Surveillance of Highway Traffic", ACM 2nd International Workshop on Video Surveillance & Sensor Networks.

[6] Lee J., Huang R., Vaughn A., Xiao X., Hedrick J.K., Zennaro M., and Sengupta R., “Strategies of Path-Planning for a UAV to Track a Ground Vehicle”, AINS 2003, Menlo Park, CA, June 2003.

[7] Shastry, A., and Schowengerdt, R., “Airborne Video Registration for Visualization and Parameter Estimation of Traffic Flows”, Pecora 15/Land Satellite Information Information IV/ISPRS Commission I/FIEOS 2002 Conference Proceedings, 2002